Xp11 translocation renal cell carcinoma with morphological features mimicking multilocular cystic renal neoplasm of low malignant potential: a series of six cases with molecular analysis

Yankun Song,[1] Xiaoxue Yin,[1] Qiuyuan Xia,[2] Linmao Zheng,[1] Jin Yao,[3] Hao Zeng,[4] Ling Nie,[1] Jing Gong,[1] Qiao Zhou,[1] Ni Chen [1]

[1]Pathology, West China Hospital, Sichuan University, Chengdu, China
[2]Pathology, Nanjing Jinling Hospital, Nanjing, China
[3]Radiology, West China Hospital, Sichuan University, Chengdu, China
[4]Urology, West China Hospital, Sichuan University, Chengdu, China

Correspondence to
Dr Ni Chen, Pathology, West China Hospital, West China Medical School, Sichuan University, Chengdu 610041, China; chenni1@163.com

YS and XY are joint first authors.

Received 21 April 2020
Revised 12 June 2020
Accepted 14 June 2020
Published Online First 22 July 2020

To cite: Song Y, Yin X, Xia Q, *et al*. *J Clin Pathol* 2021;**74**:171–176.

ABSTRACT

Aims Xp11 translocation renal cell carcinoma (RCC) is a distinctive subtype of RCC with *TFE3* (Transcription Factor Binding to IGHM Enhancer 3) gene rearrangement. The gross features in most Xp11 translocation RCCs closely resemble clear cell RCCs. In this study, we report six cases of Xp11 translocation RCCs with a unique multicystic architecture, reminiscent of multilocular cystic renal cell neoplasm of low malignant potential (MCRN-LMP).

Methods and results Microscopically, the renal mass was well circumscribed with multilocular cystic architecture. The cyst walls and septa were mostly lined by a single layer of cells with clear cytoplasm and low-grade nuclei, reminiscent of MCRN-LMP. Psammoma bodies were detected in four cases. One particular patient was misdiagnosed with benign cysts in local hospitals and led to second operation. Tumour cells were settled according to the track of the first surgical procedure. *TFE3* fluorescence in situ hybridization (FISH) assay confirmed the diagnosis of Xp11 translocation RCCs. FISH and RNA sequencing analyses confirmed *MED15-TFE3* gene fusion in all six cases. Respective patients were alive, without any recent evidence of disease recurrence and/or metastasis.

Conclusions Here, we introduce a relatively inertia-variant of Xp11 translocation RCC which mimics MCRN-LMP. The distinctive morphological condition is linked to *MED15-TFE3* gene fusion. In fact, renal neoplasms with morphological features of MCRN-LMP, especially those containing psammoma bodies, should be routinely evaluated for evidence of *TFE3* gene rearrangements.

INTRODUCTION

Xp11 translocation renal cell carcinoma (RCC) is a distinctive subtype of RCC that affects more children and young adults. This condition is characterised by a chromosome translocation involving the Xp11 breakpoint, which results in gene fusion events involving *TFE3* (Transcription Factor Binding to IGHM Enhancer 3). The *TFE3* gene has been found to rearrange with a representative number of genes. *ASPSCR1*, *PRCC* and *SFPQ* are the most common gene partners.[1–3] Other genes, such as *NONO*, *CLTC*, *PARP14*, *LUC7L3*, *KHSPR*, *RBM10*, *DVL2*, *GRIPAP1*, *ARID1B*, *NEAT-1*, *KAT6A*, *EWRS1* and *MED15*, have also been involved in *TFE3* rearrangement.[4–14] Distinct gene fusions in Xp11 translocation RCC appear to be associated with different morphological features.[7]

The gross features of the Xp11 translocation RCC can closely resemble those of clear cell RCC. Gross examination often reveals a tan-yellow tumour (also impacted by necrosis and haemorrhage), and some cases appear largely papillary.[15] The most distinctive histological pattern of the Xp11 translocation RCC relates to a neoplasm composed of voluminous clear cytoplasm or a mixture of clear and eosinophilic cytoplasm with papillary, alveolar or nested architecture. Abundant psammoma bodies can be easily seen in this kind of tumour. Still, the morphological spectrum of Xp11 translocation RCCs has been expanded to include cases reminiscent of (1) collecting duct carcinoma, (2) mucinous tubular and spindle cell carcinoma and (3) oncocytoma,[15] also can mimic the recently described entity clear cell papillary RCC.[16]

Cystic degeneration is frequently seen in RCC. Nevertheless, 'cystic RCC' does not represent a specific entity but rather reflects a degenerative or unusual growth pattern of a tumour belonging to one of the recognised RCC subtypes. According to the 2004 WHO classification, one specific cystic tumour (ie, multilocular cystic renal cell carcinoma) has been considered a distinct subtype of clear cell RCC. It has been renamed by the 2016 WHO classification as multilocular cystic renal cell neoplasm of low malignant potential (MCRN-LMP).

Some Xp11 translocation RCCs containing extensive cystic appearance have been described[12 17–19] but still, their biological behaviour is mostly unknown. Here, we report six cases of Xp11 translocation RCCs, confirmed by *TFE3* fluorescence in situ hybridization (FISH) analysis, with general and microscopic features related to MCRN-LMP. All cases were confirmed by FISH and/or RNA sequencing to harbour *MED15-TFE3* fusion, which represent a morphological variant of *TFE3* translocation RCC. As a complete cystic lesion, one particular case (case number 6) was misdiagnosed as a benign cyst and, as a result, it was previously submitted to laparoscopic renal cyst decortication (LRCD), leading to tumour cell seeding across the track of the first surgical procedure.

Table 1 Clinical features of this series of cases

Case	Sex	Age (years)	Size (cm)	Treatment	Follow-up (months)	
				First operation	Reoperation	
1	M	40	4.0	PN	–	46, NED
2	F	51	3.6	PN	–	38, NED
3	M	49	3.0	RN	–	54, NED
4	M	47	5.8	PN	–	8, NED
5	F	28	3.0	PN	–	19, NED
6	F	32	3.1	LRCD	3 months after the first operation, RN	56, NED

LRCD, laparoscopic renal cyst decortication; NED, no evidence of disease; PN, partial nephrectomy; RN, radical nephrectomy.

Case presentation

The initial case set included 29 tumours that morphologically showed like MCRN-LMP, which were retrospectively identified from the surgical pathology archival files of West China Hospital from 2014 to 2019. *TFE3* immunostaining was performed in all these cases, and six cases with strong nuclear *TFE3* immunoreactivity were included in this study. The clinicopathological features, treatment and follow-up data were recorded accordingly (table 1). This series of patients (three of each gender) were ranged in age from 28 to 51 years old. Tumour size ranged from 3.0 to 5.8 cm in its greatest dimension. Tumours were entirely embedded for diagnosis.

Cases 1 to 4 were referred to our hospital due to the presence of kidney cystic mass, as revealed by physical examination. Haematuria and/or history of other significant diseases were absent. CT scanning revealed a complete or mostly cystic mass located in the kidney (case 1, figure 1A). Partial nephrectomy was performed in cases 1, 2 and 4, while a radical nephrectomy was performed in case 3. Case 5 was admitted to our hospital due to adrenal pheochromocytoma and ipsilateral renal cyst. Both adrenal mass and renal cyst were removed during the same surgical procedure. Case 6 was diagnosed as a complex renal cyst and initially submitted to LRCD in a local hospital. A tissue slide was examined in our hospital and then diagnosed as Xp11 translocation RCC. A second operation for radical nephrectomy with lymph node dissection was further performed.

METHODS

Immunohistochemistry

The following primary antibodies (and respective dilutions) were used for immunohistochemistry (IHC) analysis: AMACR (mouse monoclonal, 1:100; DakoCytomation), carbonic anhydrase IX (CAIX) (mouse monoclonal, 1:100; Zymed, San Francisco, California, USA), CD10 (mouse monoclonal, 1:100; DakoCytomation), cytokeratin 7 (mouse monoclonal, 1:100; Zymed), epithelial membrane antigen (EMA: mouse monoclonal, 1:100; DakoCytomation), HMB45 (mouse monoclonal, 1:100; DakoCytomation), PAX8 (mouse monoclonal, 1:100; Zymed), RCC (mouse monoclonal, 1:100; NeoMarkers), *TFE3* (mouse monoclonal, 1:200, Maixin) and vimentin (mouse monoclonal, 1:100; DakoCytomation). Routine 4 µm sections were prepared from formalin-fixed, paraffin-embedded tissue blocks on 3-aminopr opyltriethoxysilane-treated glass slides. Antigen retrieval was achieved by boiling the sections in 0.01 mol/L citrate buffer (pH 6.0) in a high-pressure cooker for 3 min. Immunohistochemical staining was performed according to the manufacturer's protocol (Envision kit, DakoCytomation).

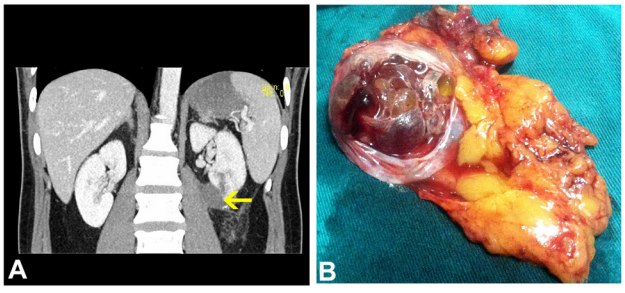

Figure 1 CT scan revealed a complete cystic mass (arrow) in the lower pole of the left kidney in case 1 (A). Gross appearance of case 1, consisting exclusively of variably sized cysts separated by thin septa and filled with clear or serous fluid (B).

FISH analysis

Formalin-fixed, paraffin-embedded tissue sections were examined by interphase FISH to investigate *TFE3* rearrangement(s). Therefore, FISH analysis was performed by using a *TFE3* dual-colour break-apart probe (Anbiping company, Guangzhou, China) and a *TFE3-MED15* gene fusion probe (provided by Dr Qiu Rao, Department of Pathology at Nanjing Jinling Hospital, Nanjing, China). Briefly, paraffin sections were deparaffinised, permeabilised and hybridised. Samples with relevant signal in more than 90% of nuclei were considered acceptable. Slides were evaluated by two independent investigators. At least 100 interphase nuclei were analysed. Based on this approach, *TFE3* gene rearrangement would lead to a break apart of the normal fused green-orange signals, resulting in only one green/one orange break-apart signal pattern in male patients, and one green/one orange break apart signal, with one remaining normal green-orange fusion signal, in female patients (normal male or female cells typically show one or two fused signals, respectively). A colocalised signal represented a fusion between *MED15* and *TFE3* gene, as described previously.[12] A positive score was reported when >10% of the nuclei from tumour cells showed evidence of *TFE3* gene rearrangement or *TFE3-MED15* gene fusion.

RNA sequencing

Total RNA was extracted from formalin-fixed paraffin-embedded samples using the RNeasy kit (QIAGEN). Next-generation sequencing and targeted RNA sequencing analysis were performed according to the manufacturer's recommendation, using a HiSeq next-generation sequencer (Illumina, San Diego, California, USA) at GloriousMed Technology (Beijing, China).

RESULTS

Gross examination indicated kidney masses mostly multicystic, with a circumscribed appearance and diameter of 3.0–5.8 cm (case 1, figure 1B). Cross-sectional analysis revealed a multicystic and well-delimited lesion, which could be subdivided by thin membranous and fibrous septa into various sized and roundish cavities. No solid nodule was detected in any of the cases. Tumours *were entirely embedded for diagnosis*.

The pathological features of each patient case are summarised in table 2. Microscopically, the respective kidney masses were well delimited by a fibrous tissue, and tumours showed a multilocular cystic architecture. Cyst walls and septa were mostly lined by a single cell layer with clear to eosinophilic cytoplasm and uniform round nuclei with small and modest nucleoli (WHO/ISUP grade 1 or 2). These tissue and cellular characteristics were reminiscent

Table 2 Morphological features and immunophenotype of this series of cases

Immunophenotype								Morphological features				
Case	*TFE3*	PAX8	EMA	CK7	CAIX	MART-1	CD10	RCC	ISUP grading	Psammoma bodies	Necrosis	Pigment
1	+	+	–	–	–	+	+	+	2	–	–	–
2	+	+	–	–	–	–	–	NA	2	–	–	–
3	+	+	–	–	–	–	–	+	2	+	–	–
4	+	+	–	–	–	–	–	NA	1	+	–	–
5	+	+	–	–	–	+	–	NA	1	+	–	–
6	+	+	–	–	–	+	+	+	2	+	–	–

CAIX, carbonic anhydrase IX; EMA, epithelial membrane antigen; NA, not available; RCC, renal cell carcinoma; TFE3, Transcription Factor Binding to IGHM Enhancer 3.

of MCRN-LMP (figure 2A–D). Entrapped non-neoplastic renal tubules were noticed between tumour cells in case 4 (figure 2E). Psammoma bodies were also observed in four cases (figure 2F, table 2). Distinctive multifocal psammoma bodies and large calcified foci were seen in case 4. Scattered and small psammoma bodies were observed in the cyst wall of the other three cases (cases 3 and 5–6). No pigment, necrosis and mitosis were observed. A complete cystic mass was originally detected in case 6 (figure 3A) and, as a result, the patient was accepted for LRCD in the local hospital. Biopsy from limiting tissue taken from cyst decortication showed the same morphological features as for the other cases (figure 3B–C). It was regrettable that, based on the tissue samples derived from the secondary radical nephrectomy of case 6, tumour cells grew in the fibre spacing and adipose tissue from the Gerota's fascia along the track of the first surgical procedure (figure 3D–F).

IHC analysis of *TFE3* protein showed a strong nuclear staining in tumour cells (figure 4A). PAX8 staining was also diffusely positive (figure 4B). The melanocytic markers MART-1(figure 4C) and CD10 (figure 4D) were positive in some of the cases (table 2). In contrast, tumour cells showed lack of expression for CK7, EMA and CAIX. IHC results were summarised in table 2.

The FISH assay with break-apart *TFE3* probe showed different patterns of detection in male and female patients. In male patients, a positive result included a single pair of separated green and red signals or, alternatively, a single green or red signal due to section truncation (figure 5A). Conversely, in female patients, a positive result included one fused signal (representing the unrelated copy of the X chromosome) and an additional pair of separated green and red signals or, alternatively, a single green or red signal due to section truncation (figure 5B). All cases were

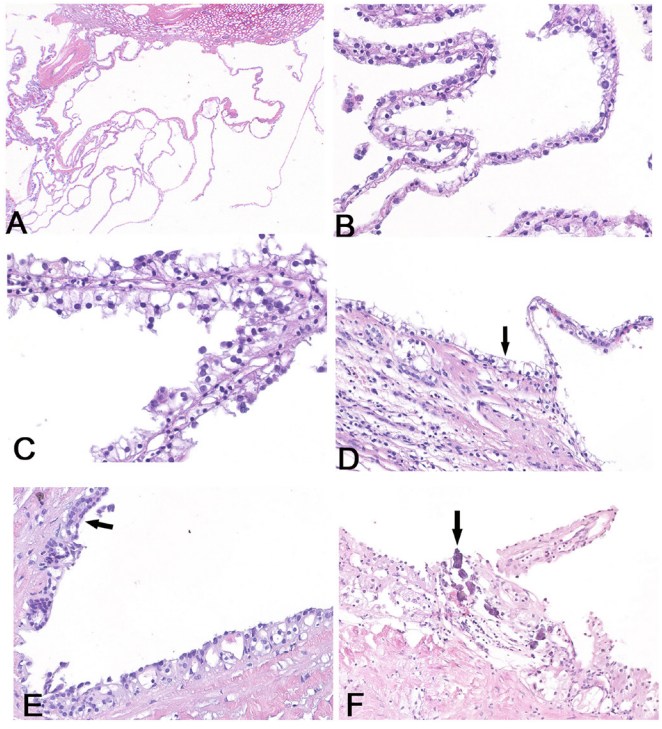

Figure 2 Whole-mount section of case 2, showing multicystic architecture without solid nodules (A). Middle power histological features of case 2 were shown (B). The septa lined by a single layer of clear cells with low-grade nuclei were detected by high power view (C). The inner wall of the capsule was lined with a single layer of clear cells (arrow) in case 6 (D). Entrapped non-neoplastic renal tubules (E) and psammoma bodies (F) were shown.

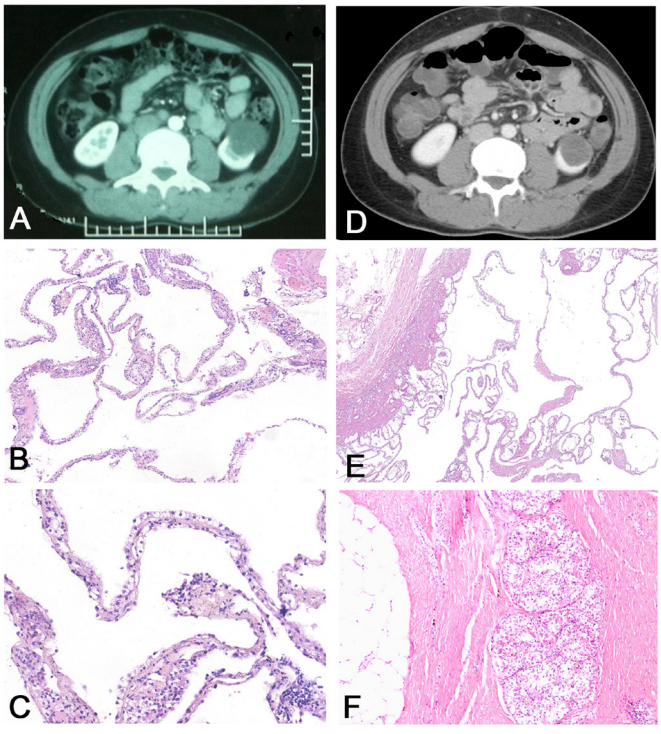

Figure 3 CT imaging (A) and multicystic histological features (B and C) of the first operation of case 6. Psamomma bodies were clearly observed (B). CT imaging before the second operation showed a complex cystic mass (D). Low power view of the slide also showed a multicystic architecture without solid composition in case 6 (E). Tumour cells were observed growing in the fibre spacing and adipose tissue of the Gerota's fascia through the track of the first operation (F).

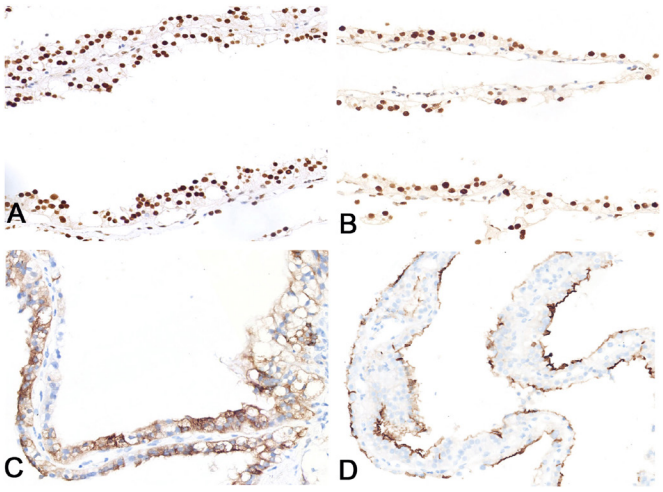

Figure 4 Immunohistochemistry assays indicating positivity for *TFE3* (A), PAX8 (B), MART-1 (C) and CD10 (D) in the clear epithelial cell lining. TFE3, Transcription Factor Binding to IGHM Enhancer 3.

confirmed by FISH assay to acquire *TFE3* gene rearrangement. Altogether, these findings led to the diagnosis of Xp11 translocation RCCs containing features of MCRN-LMP. FISH analysis of *MED15-TFE3* gene fusion was performed in four cases (cases 1 and 4–6). All four cases were confirmed to harbour *MED15-TFE3* gene fusion (figure 5C–D, table 3).

RNA sequencing results were listed in table 3. According to these data, four cases (cases 1 to 4) demonstrated a rare *TFE3*-associated gene fusion (ie, *MED15-TFE3*). In contrast, no gene

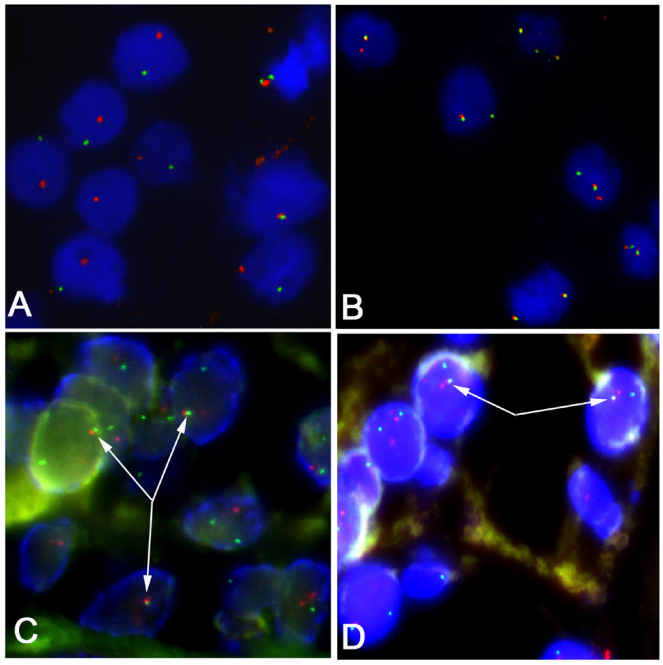

Figure 5 FISH analysis showing tumour cells in Xp11 translocation RCCs harbouring one green/one orange break-apart signal pattern in a male patient (A), and one green/one orange break-apart signal with one remaining normal green-orange fusion signal in a female patient (B). *MED15-TFE3* gene fusion was identified by fusion FISH assay. Arrows show the fusion signals (C and D). FISH, fluorescence in situ hybridization RCC, renal cell carcinoma.

Table 3 Morphology and molecular changes in *MED15-TFE3* RCCs reported

			Molecular test		
Author	N	Morphology	*TFE3* FISH	Fusion FISH	RNA-seq
Classe *et al*[9]	1	Solid and cystic	+	NA	*MED15-TFE3*
Wang *et al*[12]	2	Extensively cystic	+	*MED15-TFE3*	*MED15-TFE3*
	3	Tubular, papillary, solid	+	*MED15-TFE3*	*MED15-TFE3*
	4	Extensively cystic	+	*MED15-TFE3*	*MED15-TFE3*
	5	Extensively cystic	+	*MED15-TFE3*	NA
	6	Cystic, papillary, solid	+	*MED15-TFE3*	NA
Pei *et al*[13]	7	Papillae and granular cytoplasm	NA	NA	*MED15-TFE3*
Ye *et al*[27]	8	Cystic and solid	+	NA	*MED15-TFE3*
Song *et al* (the present study)	9	MCRN-LMP-like	+	*MED15-TFE3*	*MED15-TFE3*
	10	MCRN-LMP-like	+	NA	*MED15-TFE3*
	11	MCRN-LMP-like	+	NA	*MED15-TFE3*
	12	MCRN-LMP-like	+	*MED15-TFE3*	*MED15-TFE3*
	13	MCRN-LMP-like	+	*MED15-TFE3*	NA
	14	MCRN-LMP-like	+	*MED15-TFE3*	NA

FISH, fluorescence in situ hybridization; MCRN-LMP, multilocular cystic renal cell neoplasm of low malignant potential; NA, not available; RCC, renal cell carcinoma; TFE3, Transcription Factor Binding to IGHM Enhancer 3.

partners were identified in cases 5 and 6, possibly due to the limited number of tumour cells to obtain good quality RNA.

Follow-up data were available for all six cases (table 1). Respective patients were alive, without any recent evidence of disease recurrence and/or metastasis.

DISCUSSION

According to previous studies, the incidence of Xp11 translocation RCC varies between 1% and 4%. Xp11 translocation RCC occurs predominantly in children and young adults, but may also occur in older people.[7 12 17–22] In fact, the mean age of the cases here was 41.2 years, which seemed slightly older than the mean age of most patients affected by Xp11 translocation RCCs.

Several morphological variations had been described in Xp11 translocation RCCs. The architectures of the tumours can be predominantly nested, papillary or both. Tumours are predominantly composed of clear cells or, alternatively, eosinophilic and clear cells with high nuclear grade.[18 19 22] Here, we presented a group of cases showing a multicystic architecture, composed of thin fibrous septa with clear cytoplasm and uniform round nuclei and small inconspicuous nucleoli, with or without psammoma bodies. The general microscopic features characterised this lesion quite reminiscent of MCRN-LMP and, therefore, expanded our understanding of the heterogeneity of Xp11 translocation RCCs.

Typically, Xp11 translocation RCCs poorly express epithelial immunohistochemical markers such as cytokeratins and EMA. In contrast, most of Xp11 translocation RCCs consistently express cathepsin K, RCC, CD10, PAX2 and PAX8. Some conditions also express melanocytic markers, such as Melan A and HMB45.[23] Importantly, the strong nuclear *TFE3* immunoreactivity appears to be the most sensitive and specific immunostaining marker for Xp11 translocation RCCs.[24] Besides gene translocation, tumours with *TFE3* amplification can also lead to a strong nuclear immunoreactivity for *TFE3*.[25] Nevertheless, weak or absent TFE3 immunostaining has also been reported in Xp11 translocation RCCs.[19] Break-apart FISH assay that focused on the detection of *TFE3* rearrangement has been developed for formalin-fixed,

paraffin-embedded tissues. This assay is sensitive and specific for most of neoplasms harbouring *TFE3* gene fusions.[18 19 25] According to the type of probe used, FISH assays can define specific partners of *TFE3* rearrangement.[7 22] Our current cases presented atypical histological morphology, with standard immunophenotype and molecular changes of Xp11 translocation RCCs, which confirmed the diagnosis of MCRN-LMP-like Xp11 translocation RCCs.

The first fusion partner of *TFE3* was cloned in 1996, which was found to fuse the *TFE3* gene on Xp11.2 to the *PRCC* gene located at 1q21.2.[1 26] Since then, various other *TFE3* fusion partners have been described, including *ASPSCR1*, *SFPQ*, *NONO*, *CLTC*, *PARP14*, *LUC7L3*, *KHSPR*, *RBM10*, *DVL2*, *GRIPAP1*, *ARID1B*, *MED15*, *EWRS1*, *NEAT-1* and *KAT6A*.[1–8 10–14] In addition, *MED15* gene fusion was recently identified.[12] So far, only eight cases of *MED15-TFE3* RCC have been reported (table 3). The first case was reported by Classe *et al* with a mixed papillary, solid and cystic structure.[9] Wang and colleagues reported five cases of *MED15-TFE3* RCC. Three of these cases presented an extensive cystic architecture, while one case presented distinct cystic areas, merged with papillary and solid structures, and the remaining case was related to advanced metastasis with mixed tubular, papillary and solid nested patterns.[12] Then, Pei *et al* reported a *MED15-TFE3* RCC showing papillae and granular cytoplasm.[13] Most recently, Ye *et al* reported a new case showing solid and small nest pattern.[7 27] In this study, *MED15-TFE3* fusion was confirmed in all six MCRN-LMP-like Xp11 translocation RCCs. Therefore, summarised from the limited cases, *MED15-TFE3* RCCs can present as cystic, solid and papillary structures, but MCRN-LMP-like Xp11 translocation RCCs could be linked to *MED15-TFE3* gene fusion.

The clinical outcome of Xp11 translocation RCCs is highly variable. In particular, Xp11 translocation RCCs tend to develop in young patients with lymph node metastasis, while children with locally advanced disease appear to have a favourable prognosis.[21] Advanced staging, older age at diagnosis and *ASPSCR1-TFE3* fusion subtype are predictors of poor disease outcome.[21] Unfortunately, targeted therapy approaches have not been broadly effective to alleviate this condition. So far, surgical procedures seem to be the sole effective therapy for Xp11 translocation RCC. Still, few prognostic analyses have been reported in regard to multicystic Xp11 translocation RCCs. Therefore, further studies are needed to better assess treatment and long-term prognosis of Xp11 translocation RCCs . In the present study, tumour, node, metastases (TNM) staging of all patient cases was pT1N0M0 at the time of first operation. No evidence of disease recurrence and metastasis was reported between 8-month and 56-month follow-up, even on tumour cell implantation along the track of the surgical procedure (case 6), indicating that tumourigenesis had a relative inert biological behaviour. According to the five cases of *MED15-TFE3* RCCs reported by Wang *et al*, one patient with mixed tubular, papillary and solid nested patterns developed lung metastasis after 15 years.[12] So, a differential diagnosis of *MED15-TFE3* RCC with multilocular cystic is of seminal importance.

At present, a total of nine cases morphologically mimicking MCRN-LMP (including three reported cases and our six cases) were identified on the diagnosis of Xp11 translocation RCCs.[12] *MED15-TFE3* gene fusion was confirmed in all nine cases by FISH and/or RNA sequencing. Our findings further suggested that this tumour may be present as a low-grade morphological variant of *TFE3* translocation RCCs, with relatively good prognosis. On the other hand, this tumour variant should be submitted to a detailed preoperative imaging assessment to avoid the inaccurate detection of a benign cyst, especially that this tumour typically has an aggressive behaviour on implantation according to the surgical track. Renal neoplasms with the morphology of multilocular cystic renal cell neoplasm of low malignant potential (especially those including psammoma bodies and negative CAIX staining and/or MART-1 positivity) should be routinely evaluated for evidence of *TFE3* gene rearrangements.

Take home messages

- In this study, we reported a series of six Xp11 translocation renal cell carcinomas (RCCs) with morphological features mimicking multilocular cystic renal cell neoplasm of low malignant potential (MCRN-LMP).
- Psammoma bodies and atypical immunohistochemical results (negative CAIX staining and/or MART-1 positivity) may be helpful clues to the diagnosis of this entity.
- The distinctive morphological condition is linked to *MED15-TFE3* gene fusion.
- The behaviour of Xp11 translocation RCCs with morphological features mimicking MCRN-LMP appears indolent.

Handling editor Runjan Chetty.

Contributors YS and XY collected the patients and did the TFE3 FISH and wrote the paper; QX performed the TFE3-MED15 fusion FISH; JY supplied the radiology image; LZ and LN did the immunohistochemistry; HZ and JG organised the clinical data; QZ and NC organised and modified the paper.

Funding Supported by grants from the National Natural Science Foundation of China (NSFC 81872107, 81872108).

Competing interests None declared.

Patient consent for publication Not required.

Ethics approval This study was approved by the Institute Research Ethics Committee of West China Hospital.

Provenance and peer review Not commissioned; externally peer reviewed.

Data availability statement All data relevant to the study are available from the surgical pathology archival files of West China Hospital from 2014-2019. This study is approved by the Institute Research Ethics Committee of West China Hospital.

ORCID iD

Ni Chen http://orcid.org/0000-0002-0628-0723

REFERENCES

1 Weterman MA, Wilbrink M, Geurts van Kessel A. Fusion of the transcription factor TFE3 gene to a novel gene, PRCC, in t(X;1)(p11;q21)-positive papillary renal cell carcinomas. *Proc Natl Acad Sci U S A* 1996;93:15294–8.
2 Clark J, Lu YJ, Sidhar SK, *et al*. Fusion of splicing factor genes PSF and NONO (p54NRB) to the TFE3 gene in papillary renal cell carcinoma. *Oncogene* 1997;15:2233–9.
3 Argani P, Antonescu CR, Illei PB, *et al*. Primary renal neoplasms with the ASPL-TFE3 gene fusion of alveolar soft part sarcoma: a distinctive tumor entity previously included among renal cell carcinomas of children and adolescents. *Am J Pathol* 2001;159:179–92.
4 Argani P, Lui MY, Couturier J, *et al*. A novel CLTC-TFE3 gene fusion in pediatric renal adenocarcinoma with t(X;17)(p11.2;q23). *Oncogene* 2003;22:5374–8.
5 Malouf GG, Su X, Yao H, *et al*. Next-Generation sequencing of translocation renal cell carcinoma reveals novel RNA splicing partners and frequent mutations of chromatin-remodeling genes. *Clin Cancer Res* 2014;20:4129–40.
6 Huang W, Goldfischer M, Babayeva S, *et al*. Identification of a novel PARP14-TFE3 gene fusion from 10-year-old FFPE tissue by RNA-seq. *Genes Chromosomes Cancer* 2015;54:500–5.
7 Argani P, Zhong M, Reuter VE, *et al*. TFE3-Fusion variant analysis defines specific clinicopathologic associations among Xp11 translocation cancers. *Am J Surg Pathol* 2016;40:723–37.
8 Argani P, Zhang L, Reuter VE, *et al*. RBM10-TFE3 renal cell carcinoma: a potential diagnostic pitfall due to cryptic intrachromosomal Xp11.2 inversion resulting in false-negative TFE3 fish. *Am J Surg Pathol* 2017;41:655–62.

9 Classe M, Malouf GG, Su X, *et al*. Incidence, clinicopathological features and fusion transcript landscape of translocation renal cell carcinomas. *Histopathology* 2017;70:1089–97.
10 Pivovarcikova K, Grossmann P, Alaghehbandan R, *et al*. TFE3-Fusion variant analysis defines specific clinicopathologic associations Amog Xp11 translocation cancers. *Am J Surg Pathol* 2017;41:138–40.
11 Xia Q-Y, Wang Z, Chen N, *et al*. Xp11.2 translocation renal cell carcinoma with NONO-TFE3 gene fusion: morphology, prognosis, and potential pitfall in detecting TFE3 gene rearrangement. *Mod Pathol* 2017;30:416–26.
12 Wang X-T, Xia Q-Y, Ye S-B, *et al*. Rna sequencing of Xp11 translocation-associated cancers reveals novel gene fusions and distinctive clinicopathologic correlations. *Mod Pathol* 2018;31:1346–60.
13 Pei J, Cooper H, Flieder DB, *et al*. NEAT1-TFE3 and KAT6A-TFE3 renal cell carcinomas, new members of MIT family translocation renal cell carcinoma. *Mod Pathol* 2019;32:710–6.
14 Fukuda H, Kato I, Furuya M, *et al*. A novel partner of TFE3 in the Xp11 translocation renal cell carcinoma: clinicopathological analyses and detection of EWSR1-TFE3 fusion. *Virchows Arch* 2019;474:389–93.
15 Argani P. Mit family translocation renal cell carcinoma. *Semin Diagn Pathol* 2015;32:103–13.
16 Parihar A, Tickoo SK, Kumar S, *et al*. Xp11 translocation renal cell carcinoma morphologically mimicking clear cell-papillary renal cell carcinoma in an adult patient: report of a case expanding the morphologic spectrum of Xp11 translocation renal cell carcinomas. *Int J Surg Pathol* 2015;23:234–7.
17 Suzigan S, Drut R, Faria P, *et al*. Xp11 translocation carcinoma of the kidney presenting with multilocular cystic renal cell carcinoma-like features. *Int J Surg Pathol* 2007;15:199–203.
18 Green WM, Yonescu R, Morsberger L, *et al*. Utilization of a TFE3 break-apart fish assay in a renal tumor consultation service. *Am J Surg Pathol* 2013;37:1150–63.
19 Rao Q, Williamson SR, Zhang S, *et al*. Tfe3 break-apart fish has a higher sensitivity for Xp11.2 translocation-associated renal cell carcinoma compared with TFE3 or cathepsin K immunohistochemical staining alone: expanding the morphologic spectrum. *Am J Surg Pathol* 2013;37:804–15.
20 Sukov WR, Hodge JC, Lohse CM, *et al*. Tfe3 rearrangements in adult renal cell carcinoma: clinical and pathologic features with outcome in a large series of consecutively treated patients. *Am J Surg Pathol* 2012;36:663–70.
21 Ellis CL, Eble JN, Subhawong AP, *et al*. Clinical heterogeneity of Xp11 translocation renal cell carcinoma: impact of fusion subtype, age, and stage. *Mod Pathol* 2014;27:875–86.
22 Rao Q, Shen Q, Xia Q-yuan, *et al*. PSF/SFPQ is a very common gene fusion partner in TFE3 rearrangement-associated perivascular epithelioid cell tumors (PEComas) and melanotic Xp11 translocation renal cancers: clinicopathologic, immunohistochemical, and molecular characteristics suggesting classification as a distinct entity. *Am J Surg Pathol* 2015;39:1181–96.
23 Argani P, Hicks J, De Marzo AM, *et al*. Xp11 translocation renal cell carcinoma (RCC): extended immunohistochemical profile emphasizing novel RCC markers. *Am J Surg Pathol* 2010;34:1295–303.
24 Argani P, Lal P, Hutchinson B, *et al*. Aberrant nuclear immunoreactivity for TFE3 in neoplasms with TFE3 gene fusions: a sensitive and specific immunohistochemical assay. *Am J Surg Pathol* 2003;27:750–61.
25 Macher-Goeppinger S, Roth W, Wagener N, *et al*. Molecular heterogeneity of TFE3 activation in renal cell carcinomas. *Mod Pathol* 2012;25:308–15.
26 Sidhar SK, Clark J, Gill S, *et al*. The t(X;1)(p11.2;q21.2) translocation in papillary renal cell carcinoma fuses a novel gene PRCC to the TFE3 transcription factor gene. *Hum Mol Genet* 1996;5:1333–8.
27 Ye H, Qin S, Li N, *et al*. A rare partner of TFE3 in the Xp11 translocation renal cell carcinoma: clinicopathological analyses and detection of MED15-TFE3 fusion. *Biomed Res Int* 2019;2019:1–8.